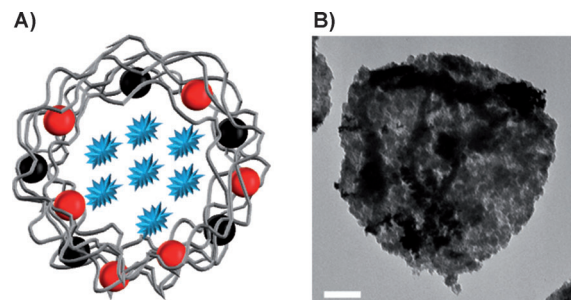


# Light-Addressable Capsules as Caged Compound Matrix for Controlled Triggering of Cytosolic Reactions\*\*

Markus Ochs, Susana Carregal-Romero, Joanna Rejman, Kevin Braeckmans, Stefaan C. De Smedt, and Wolfgang J. Parak\*

Layer-by-layer assembly was introduced almost two decades ago as a versatile technique for the construction of thin multiple-layer films composed out of polyelectrolytes.<sup>[1,2]</sup> Shortly after, the concept was extended from planar to spherical geometry, resulting in polyelectrolyte multilayer capsules.<sup>[3–5]</sup> The semipermeable wall of the capsules (with a thickness of a few nanometers)<sup>[6,7]</sup> and the cavity can be further loaded with inorganic colloidal nanoparticles (NPs) made of different materials and with multiple cargos,<sup>[8–10]</sup> respectively (Figure 1). The resulting multifunctional capsules are well-suited for in vitro delivery of cargo inside cells.<sup>[11,12]</sup> This concept has been highlighted in several recent reviews.<sup>[13–15]</sup> Meanwhile technology has advanced to a point at which these capsules could be a helpful tool for controlled multifunctional in vitro delivery. Nowadays the cavity of capsules can be loaded with a large variety of cargo. While large molecules such as proteins will be readily kept inside the cavity, small molecules need to be either linked to macromolecules such as dextran,<sup>[16]</sup> or be embedded inside micelles.<sup>[17]</sup> The micelle approach even allows for encapsulation of small hydrophobic molecules. The materials forming the polyelectrolyte wall can be chosen such that capsules internalized by cells are not degraded and preserve their cargo over weeks. Leakage of the cargo molecule is reduced and controlled release of cargo upon external stimuli can be performed.

A large number of capsules can be taken up by cells in vitro without causing acute cytotoxicity, even for capsules



**Figure 1.** A) Schematic representation of a capsule with walls produced via layer-by-layer assembly (gray). The cavity of the capsule is loaded with a cargo (blue). The wall of the capsule contains magnetic (black) and plasmonic (red) NPs. B) A representative transmission electron microscopy (TEM) image of a capsule with a large amount of magnetic  $\text{Fe}_2\text{O}_3$  and plasmonic Au NPs in its walls. The scale bar corresponds to 1  $\mu\text{m}$ .

with large sizes of around 5  $\mu\text{m}$ .<sup>[18–20]</sup> It is conceivable that if cells are exposed simultaneously to different types of capsules with similar layer composition, they will internalize them with a statistical distribution. To demonstrate this we exposed cells to a mixture of four types of capsules loaded with different fluorescently labeled dextrans emitting blue, green, red, or near-infrared light (Figure 2A) corresponding to Cascade Blue, fluorescein isothiocyanate, AlexaFluor594, and Dy647, respectively. HeLa cells were incubated with amounts of capsules equivalent to two, four, or six capsules of each color per cell for four hours. Figure 2B presents the number of capsules of each color internalized per cell. When six capsules of each color (i.e. 24 capsules in total) were added per cell, 50 % of the cells had internalized at least one capsule of each color. Contrary, when only two capsules per cell of the four kinds were added the percentage dropped to less than 20 %. These findings demonstrate the feasibility to simultaneously load cells with a variety of encapsulated cargos.

The loading of cells can be specifically directed by incorporating magnetic NPs in the wall of the capsules. This is possible since magnetic field gradients, which are created by positioning a magnet in a flow channel system, trap the capsules close to the magnet.<sup>[21]</sup> This method can ultimately be used to achieve specific capsule distribution patterns in the cell culture or in vivo for certain applications. Figure 2C,D shows the results of an experiment demonstrating the targeted deposition of differently colored capsules in a sub-millimeter pattern. A magnet with an edge length of 5 mm (ca. 1.3 T) was modified with two iron slips on top (width ca. 800  $\mu\text{m}$ ) that apply the magnetic field in the shape of two stripes underneath a flow channel, which simulates blood

[\*] M. Ochs,<sup>[†]</sup> Dr. S. Carregal-Romero,<sup>[†]</sup> Prof. W. J. Parak  
Fachbereich Physik und WZWM, Philipps Universität Marburg  
Renthof 7, 35037 Marburg (Germany)  
E-mail: wolfgang.parak@physik.uni-marburg.de

Dr. S. Carregal-Romero<sup>[†]</sup>  
Bionand. Severo Ochoa 35, 29590 Málaga (Spain)

Dr. J. Rejman, Prof. K. Braeckmans, Prof. S. C. De Smedt  
Laboratory of General Biochemistry and Physical Pharmacy  
Ghent University  
Harelbekestraat 72, Ghent (Belgium)

Prof. K. Braeckmans  
Center for Nano and Biophotonics, Ghent University  
Harelbekestraat 72, Ghent (Belgium)

[†] These authors contributed equally to this work.

[\*\*] This work was supported by BMBF/ERANET (project Nanosyn) and the DFG (project PA794/11.1). We acknowledge technical discussions with Drs. Rafael Fernandez Chacón, Loretta del Mercato, Arnold Grünweller, Roland Hartmann, Pilar Riveral Gil and Gleb B. Sukhorukov.



Supporting information for this article is available on the WWW under <http://dx.doi.org/10.1002/anie.201206696>.

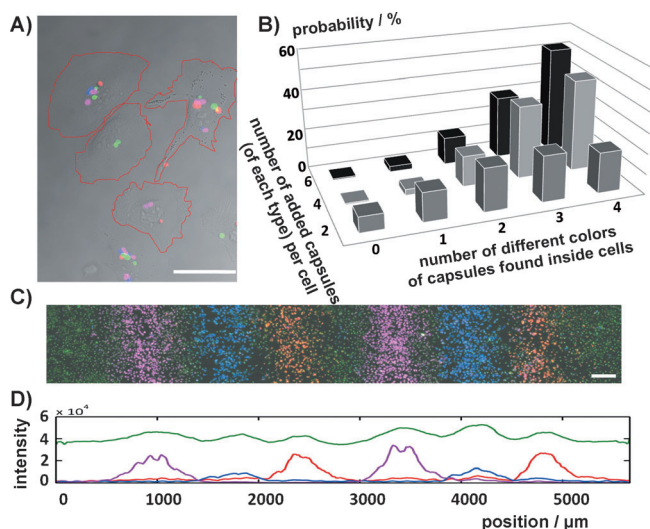


**Figure 2.** A) HeLa cells were incubated with a homogeneous mixture of fluorescent capsules in blue, green, red, and violet. An overlay of phase contrast and different fluorescence images is shown. The scale bar corresponds to 50 μm. Cell borders are indicated by red lines. B) Two, four, or six capsules of each type per cell were added to the culture medium. The probability of observing in one cell 0, 1, 2, 3, and 4 capsules of different color is plotted. C) Lateral arrangement of fluorescent capsules within a cell culture owing to magnetic guidance in a flow chamber. The scale bar corresponds to 250 μm. D) Corresponding fluorescence intensity of each color along the flow channel shown in (C). The green fluorescence signal belongs to cell staining with AlexaFluor488 useful to colocalize the fluorescent signals from capsules and cells.

stream, in which the cells were cultured. Capsules loaded with a fluorescent dye linked to dextran and magnetic NPs were added and allowed to circulate in the flow medium above the cells for ten minutes. Then the magnet was moved along the channel, and a new type of capsules loaded with another fluorophore was added to the flow medium for ten minutes. This procedure was repeated, and the magnet was moved along the channel in distance steps of 800 μm. The respective capsules were trapped close to the position of the magnet, locally concentrated, and subsequently internalized by the cells. This procedure allowed for obtaining a submillimeter resolution level of the patterns. In summary, capsules with different cargo can be directed by magnetic field gradients to specific regions of a cell culture.

Most cell types internalize capsules in a nonspecific way through different endocytotic pathways, whereby most of the capsules ultimately are located inside lysosomes.<sup>[18]</sup> Capsules modified with plasmonic NPs allow for releasing cargo from lysosomes to the cytosol by photothermal heating.<sup>[22–25]</sup> This is similar to the classical concept of light-controlled release of caged compounds (such as caged calcium) inside cells.<sup>[26]</sup> Our approach, however, allows light-controlled release of a much larger class of molecules and also subsequent release of different molecules. Moreover, the technique to open the capsules is applied on individual capsules, thereby permitting sequential opening of different capsules within one cell.<sup>[27]</sup> Local disruption of the capsule walls also leads to (transient) permeability of the membrane of the lysosomes in which the

illuminated capsules are located. Release however can be triggered in a controlled way with keeping the biological activity of the cargo molecule and with tolerable effects on cellular viability.<sup>[22,27]</sup> The appropriate intensity of the infrared laser pointer was studied previously.<sup>[22]</sup> Au NPs were loaded at high density to the capsule walls, as photothermally deposited heat increases for larger clusters.<sup>[28]</sup> Here, we demonstrate that this approach can be employed to orchestrate intracellular reactions. We have studied the triggering of an enzymatic reaction upon consecutive opening of capsules containing either the enzyme or the substrate (Figure 3). Alkaline phosphatase (enzyme) converts ELF97 phosphate (substrate) into green fluorescent ELF97 alcohol (Figure 3A). These two cargos were loaded separately in two different types of capsules and delivered into the same cell. Both capsules, which had Au NPs in their walls, were independently opened with a light pointer (intensity 3 mW μm<sup>−2</sup> for 1 s), which had been focused on the respective capsule. As a result the contents of the capsules (the enzyme or the substrate) were released into the cytosol (Figure 3). The substrate in its original state is a phosphorylated (and thus quenched) fluorophore. When only the substrate or the enzyme was released into the cytosol by light-controlled opening of one of the capsules no effect was observed (Figure 3C,F). However, after the opening of the second capsule with the complementary cargo, that is, the capsule with ELF97 phosphate or enzyme, by a second illumination, both cargos were colocated. Interaction between the substrate and the enzyme resulted in the formation of the fluorescent product, ELF97 alcohol, which precipitated at the site of the enzymatic reaction (Figure 3D,G). Production of the fluorescent product was either observed when first the substrate and second the enzyme were released or vice versa (Figure 3E–G). It is important to stress that reactions (as observed by onset of fluorescence) only occurred after successful opening of both types of capsules in the same cell.

The opening sequence mattered in the sense that the fluorescent compound formed after cleavage of the phosphate group settled down as a nonsoluble precipitate at the site where the second capsule was opened, irrespective of its content being the enzyme or the substrate. The reason for this observation is the much higher concentration of released material inside/around the last opened capsule compared to the surrounding cytosol. The efficiency of cytosolic release was around 50% (see the Supporting Information). To demonstrate that triggering of enzymatic reactions is not cell-phenotype dependent, the same experiments were performed on two more cell lines (MCF-7 and MDA-MB-231, see the Supporting Information). Finally, all these experiments demonstrate that sequential release of encapsulated materials can trigger reactions with not only one but also multiple reactive compounds inside cells.

Moreover, reaction kinetics can be recorded. The potentially strongest asset of light-mediated release lies in the possibility to employ it to follow processes in time. We demonstrate the feasibility of that approach by employing mRNA encoding green fluorescent protein (GFP). Conventionally, mRNA can be delivered to cells in the form of lipoplexes or polyplexes. These complexes are taken up by the

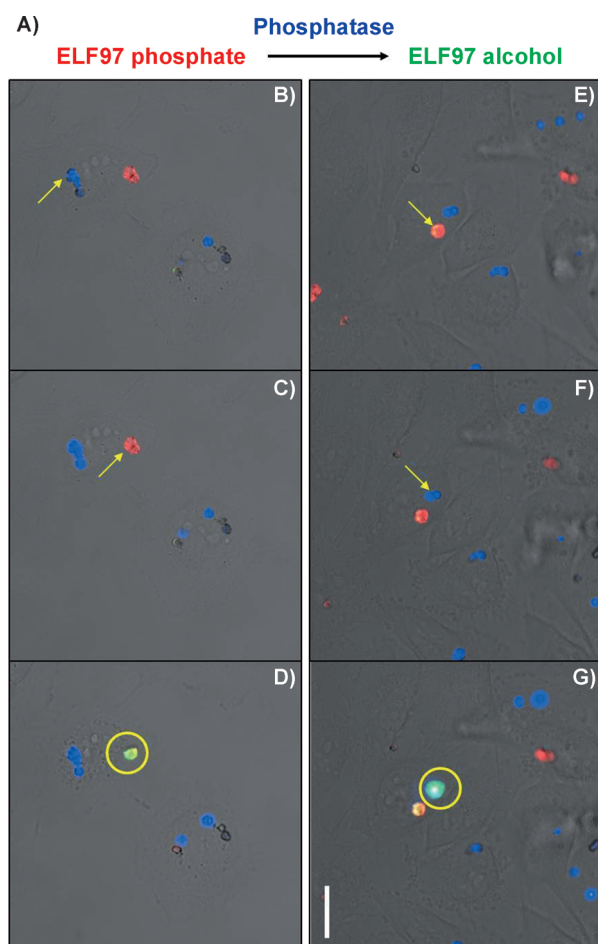


**Figure 3.** Alkaline phosphatase and ELF97 phosphate are sequentially released by light-controlled heating from capsules modified with Au NPs. A) Capsules were filled with Cascade Blue–dextran and the enzyme alkaline phosphatase (AP, blue capsules) or AlexaFluor594–dextran and the substrate ELF97 phosphate (red capsules). Fluorescently labeled dextran derivatives were co-encapsulated, because both the enzyme and the substrate are nonfluorescent by themselves. When the enzyme and the substrate interact with each other, alkaline phosphatase cleaves the phosphate group of ELF97 phosphate, thereby producing ELF97 alcohol, which is a yellow-green fluorescent precipitate. HeLa cells were incubated with both types of capsules. Only cells that contained at least one capsule of each type were selected. Capsules filled with alkaline phosphatase (B) or ELF97 phosphate (E) were first opened with a light pointer, as indicated by yellow arrows. In a next step the complementary capsules with ELF97 phosphate (C) or alkaline phosphatase (F) were opened, as indicated again by yellow arrows. Enzymatic processing of ELF97 phosphate by alkaline phosphatase led to the production of the green fluorescent product ELF97 alcohol (D, G). The scale bar corresponds to 25  $\mu\text{m}$ .

cells by means of endocytosis. To ensure protein production the complexes need to escape from the lysosome and mRNA needs to be released into the cytosol to produce the encoded protein (Figure 4). The process can be monitored by plotting GFP fluorescence versus time. If mRNA is conventionally delivered by cationic lipids or polymers, the observed protein production kinetics are a convolution of three distinct processes: the uptake of the polyplexes/lipoplexes, their release from the lysosome to the cytosol, and translation of

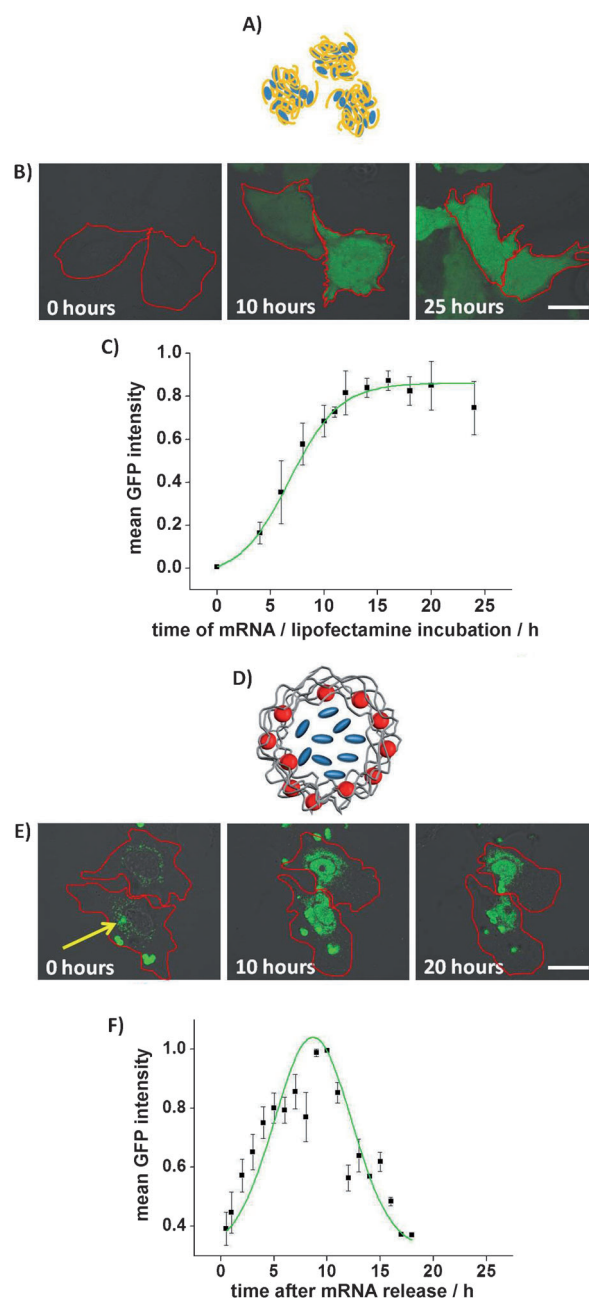


**Figure 4.** A) Lipoplexes or polyplexes (yellow) as carrier systems of mRNA encoding GFP (drawn in blue). B) Confocal images of the expression of GFP in HeLa cells using the transfection agent lipofectamine as carrier system. C) The mean fluorescence intensity per cell is plotted versus the incubation time. D) Light-responsive capsules as carrier systems of mRNA encoding GFP. Polyelectrolytes (gray), Au NPs (red), and mRNA (blue). E) Confocal images of capsules internalized by HeLa cells. Capsules were irradiated with a light pointer, as indicated by the yellow arrow. At time  $t=0$  mRNA is released into the cytosol where GFP expression started. F) The mean fluorescence intensity per cell in which one capsule was opened is plotted versus the time after capsule opening. Cell borders are indicated by red lines. Scale bars correspond to 20  $\mu\text{m}$ .

mRNA in the cytosol (Figure 4A–C). Since uptake of polyplexes/lipoplexes by cells is a statistical process over the time period of hours one cannot give the “time point zero” at



which the mRNA is actually present in the cytosol. To overcome this shortcoming, we encapsulated mRNA by using a coprecipitation method in capsules with Au NPs in their walls. The size of mRNAs is in the range of hundreds of kDa, and therefore leakage is avoided owing to steric hindrance. After internalization by cells these capsules resided in lysosomes without releasing any mRNA. Release of mRNA was triggered only by light-mediated opening of the capsules. In this way the starting point at which mRNA is first present in the cytosol can be precisely defined by the externally controlled opening process. Kinetics of protein production are thus no longer convoluted with kinetics of polyplex/lipoplex delivery and thus can be recorded independently (Figure 4D–F). Furthermore, as the release of mRNA is triggered in a “burst-like” way, there is only one distinct event in which the encapsulated mRNA is released. This event results in fluorescence intensity curves of GFP that have a Gaussian distribution with an intensity maximum around ten hours after induced release. In contrast, as shown in Figure 4C, mRNA delivered by cationic lipids is available for translation over an extended period of time. Therefore, the amount of produced GFP and subsequent fluorescence intensity is growing to a rather constant value and is stable for long time.<sup>[29]</sup> In summary, light-mediated release of encapsulated cargo can be used to directly record kinetics of reactions that are triggered by the cargo in the cytosol.

We think that one of the major advantages of the proposed method is the possibility to record kinetics of intracellular processes independently from cellular uptake processes and carrier system degradation. This method could be used for *in vitro* screening of the effects of molecular cargo released in a controlled way into the cytosol. The possibility to deliver capsules with different cargos to different parts of a cell population by using magnetic field gradients (Figure 2), combined with the ability to release the cargo of capsules individually (Figure 3), could allow for screening of the effects of several cargos and their combinations. It should be kept in mind, however, that upon light-mediated release, the membrane of the intracellular compartment in which the treated capsule is confined is locally perforated, as otherwise no release into the cytosol could occur. The applied mechanical and thermal stress can clearly lead to acute cell death. If the light energy transferred to the gold NPs and herein the resulting temperature increase is too high, treated cells die immediately. Nevertheless, if the correct parameters of light power and beam focus are found, opening of capsules is well-tolerated by cells. In particular, as our methods are based on single cells, impaired cells can be discarded from analysis. Nevertheless, as shown herein (Figure 4), our approach did not affect the biological activity of such a notoriously unstable molecule as mRNA. Nonetheless, for triggered-release experiments using the capsules as demonstrated here, interference of cytotoxic effects has to be considered, and only appropriate experiments can be chosen that have no dominant effect on the intracellular metabolism. At the current state, quantitative release is difficult to achieve owing to, for example, inhomogeneous loading of capsules with cargo and Au NPs, dependence on the illumination protocol (power density and illumination time), and incomplete release upon

light-mediated opening.<sup>[30]</sup> Thus, the system is most suited to study the kinetics of reactions in which only the mere presence of the released cargo in the cytosol but not its quantity is of relevance, as it is for example the case for the mRNA experiment shown in Figure 4. Moreover, this approach offers the greatest advantage for reactions that occur on a short time scale, that is, within a couple of hours. For much slower reactions the cargo can be introduced through classical incorporation with polyplexes/lipoplexes, because in this case the uptake and cytosolic delivery would happen on a smaller time scale than the actual reaction and thus would not interfere with the reaction kinetics. We want to emphasize in particular the possibility to release different cargos independently at designated time points within the same cell. One could think of releasing different mRNA molecules at different time points and record interactions of expressed proteins. Thus we believe that the methodology described herein already offers a great potential for numerous *in vitro* applications. *In vivo* applications would face further challenges. Even though capsules have been successfully used for vaccination purposes,<sup>[31,32]</sup> other *in vivo* applications have to cope with targeting, clearance of capsules by the immune system, and long-term cytotoxic effects. Another issue is that visible light is strongly absorbed by tissue. Even when NIR light in the “biologically friendly window” of the electromagnetic spectrum is used,<sup>[33,34]</sup> homogeneous illumination of capsules in tissue is a challenge. However, optical excitation of plasmonic NPs could be replaced by radiofrequency excitation of magnetic NPs.<sup>[35,36]</sup> Modern set-ups for magnetic-resonance imaging (MRI) already allow to follow individual cells *in vivo*. Sequential opening of different capsules might be even feasible by employing magnetic NPs of different resonance frequencies and different radiofrequency ranges, which in the future may facilitate externally triggered release from capsules also *in vivo*.

## Experimental Section

Polyelectrolyte capsules loaded with different cargo molecules in the inner cavity and magnetic and/or plasmonic nanoparticles within the wall were synthesized according to procedures described in the literature.<sup>[17,27,21]</sup> In the Supporting Information a detailed explanation of the strategies used to encapsulate the different cargos has been reported. mRNA was produced by *in vitro* transcription with appropriate plasmids (pGEM4Z/EGFP/A64 or pBlue-Luc-A50 or pCXCR4).<sup>[29]</sup> They were first purified using a QIAquick PCR purification kit (Qiagen) and linearized using restriction enzymes (Dra I for plasmid encoding firefly luciferase or Spe I for plasmid encoding GFP or Xba I for plasmid encoding CXCR4). The mRNA concentration was determined by measuring the absorbance at 260 nm. mRNA was stored in small aliquots at  $-80^{\circ}\text{C}$  at a concentration of  $1\ \mu\text{g}\ \mu\text{L}^{-1}$ . Lipofectamine lipoplexes loaded with mRNA encoding GFP (mGFP) protein were prepared by mixing Lipofectamine™ 2000 purchased from Invitrogen and mGFP in OptiMem media as it was described.<sup>[29]</sup> The basic setup for microscopic observation and experimental progress consisted of a wide-field fluorescence microscope Axiovert200M from Zeiss. The microscope was coupled with an 830 nm IR laser. The maximum light power reaching the sample plane on top of the used  $63\times/1.4$  oil immersion Plan-Apochromat objective was approximately 30 mW (continuous output). The light energy is dispersed on an oval spot of about  $6\ \mu\text{m}^2$ . With a tunable power supply the output power of the laser can be

varied smoothly from 0 to 30 mW effective light power on the sample plane. Capsules were opened upon irradiation with laser intensities between 2.5 and 3 mW  $\mu\text{m}^{-2}$  during 1–2 seconds.

Received: August 18, 2012

Revised: October 25, 2012

Published online: November 14, 2012

**Keywords:** enzyme catalysis · gene expression · nanoparticles · polymeric capsules

- [1] G. Decher, J. D. Hong, *Makromol. Chem. Macromol. Symp.* **1991**, *46*, 321.
- [2] G. Decher, J. D. Hong, J. Schmitt, *Thin Solid Films* **1992**, *210*, 831.
- [3] E. Donath, G. B. Sukhorukov, F. Caruso, S. A. Davis, H. Möhwald, *Angew. Chem.* **1998**, *110*, 2323; *Angew. Chem. Int. Ed.* **1998**, *37*, 2201.
- [4] C. S. Peyratout, L. Daehne, *Angew. Chem.* **2004**, *116*, 3850; *Angew. Chem. Int. Ed.* **2004**, *43*, 3762.
- [5] Y. Wang, A. S. Angelatos, F. Caruso, *Chem. Mater.* **2008**, *20*, 848.
- [6] T. Mauser, C. Dejumat, G. B. Sukhorukov, *J. Phys. Chem. B* **2006**, *110*, 20246.
- [7] D. G. Shchukin, G. B. Sukhorukov, H. Möhwald, *Adv. Colloid Interface Sci.* **2010**, *158*, 2.
- [8] N. A. Kotov, I. Decany, J. H. Fendler, *J. Phys. Chem.* **1995**, *99*, 13065.
- [9] F. Caruso, *Chem. Eur. J.* **2000**, *6*, 413.
- [10] D. G. Shchukin, G. B. Sukhorukov, H. Möhwald, *Angew. Chem.* **2003**, *115*, 4610; *Angew. Chem. Int. Ed.* **2003**, *42*, 4472.
- [11] A. Muñoz Javier, O. Kreft, A. Piera Alberola, C. Kirchner, B. Zebli, A. S. Sussha, E. Horn, S. Kempter, A. G. Skirtach, A. L. Rogach, J. Rädler, G. B. Sukhorukov, M. Benoit, W. J. Parak, *Small* **2006**, *2*, 394.
- [12] S. De Koker, B. G. De Geest, S. K. Singh, R. De Rycke, T. Naessens, Y. Van Kooyk, J. Demeester, S. De Smedt, J. Grooten, *Angew. Chem.* **2009**, *121*, 8637; *Angew. Chem. Int. Ed.* **2009**, *48*, 8485.
- [13] S. De Koker, R. Hoogenboom, B. G. De Geest, *Chem. Soc. Rev.* **2012**, *41*, 2867.
- [14] A. P. Esser-Kahn, S. A. Odom, N. R. Sotos, S. R. White, J. S. Moore, *Macromolecules* **2011**, *44*, 5539.
- [15] A. Johnston, G. Such, F. Caruso, *Angew. Chem.* **2010**, *122*, 2723; *Angew. Chem. Int. Ed.* **2010**, *49*, 2664.
- [16] O. Kreft, A. Muñoz Javier, G. B. Sukhorukov, W. J. Parak, *J. Mater. Chem.* **2007**, *17*, 4471.
- [17] W. Tong, Y. Zhu, Z. Wang, C. Gao, H. Mohwald, *Macromol. Rapid Commun.* **2010**, *31*, 1015.
- [18] A. Muñoz Javier, O. Kreft, M. Semmling, S. Kempter, A. G. Skirtach, O. Bruns, P. d. Pino, M. F. Bedard, J. Rädler, J. Käs, C. Plank, G. Sukhorukov, W. J. Parak, *Adv. Mater.* **2008**, *20*, 4281.
- [19] K. Wang, Q. He, X. Yan, Y. Cui, W. Qi, L. Duan, J. Li, *J. Mater. Chem.* **2007**, *17*, 4018.
- [20] B. G. De Geest, S. De Koker, G. B. Sukhorukov, O. Kreft, W. J. Parak, A. G. Skirtach, J. Demeester, S. C. De Smedt, W. E. Hennink, *Soft Matter* **2009**, *5*, 282.
- [21] B. Zebli, A. S. Sussha, G. B. Sukhorukov, A. L. Rogach, W. J. Parak, *Langmuir* **2005**, *21*, 4262.
- [22] A. Muñoz Javier, P. d. Pino, M. Bedard, A. G. Skirtach, D. Ho, G. Sukhorukov, C. Plank, W. J. Parak, *Langmuir* **2009**, *24*, 12517.
- [23] B. Radt, T. A. Smith, F. Caruso, *Adv. Mater.* **2004**, *16*, 2184.
- [24] A. G. Skirtach, A. M. Javier, O. Kreft, K. Köhler, A. P. Alberola, H. Möhwald, W. J. Parak, G. B. Sukhorukov, *Angew. Chem.* **2006**, *118*, 4728; *Angew. Chem. Int. Ed.* **2006**, *45*, 4612.
- [25] R. Palankar, A. G. Skirtach, O. Kreft, M. Bedard, M. Garstka, K. Gould, H. Mohwald, G. B. Sukhorukov, M. Winterhalter, S. Springer, *Small* **2009**, *5*, 2168.
- [26] G. C. R. Ellis-Davies, *Nat. Methods* **2007**, *4*, 619.
- [27] S. Carregal-Romero, M. Ochs, P. Rivera-Gil, C. Gana, A. M. Pavlov, G. B. Sukhorukov, W. J. Parak, *J. Controlled Release* **2012**, *159*, 120.
- [28] C. Hrelescu, J. Stehr, M. Ringler, R. A. Sperling, W. J. Parak, T. A. Klar, J. Feldmann, *J. Phys. Chem. C* **2010**, *114*, 7401.
- [29] J. Rejman, G. Tavernier, N. Bavarsad, J. Demeester, S. C. De Smedt, *J. Controlled Release* **2010**, *147*, 385.
- [30] M. F. Bedard, B. G. De Geest, A. G. Skirtach, H. Mohwald, G. B. Sukhorukov, *Adv. Colloid Interface Sci.* **2009**, *1*, 1705.
- [31] B. G. De Geest, M. A. Willart, B. N. Lambrecht, C. Pollard, C. Vervaet, J. P. Remon, J. Grooten, S. De Koker, *Angew. Chem.* **2012**, *124*, 3928; *Angew. Chem. Int. Ed.* **2012**, *51*, 3862.
- [32] M.-L. De Temmerman, J. Rejman, J. Demeester, D. J. Irvine, B. Gander, S. C. De Smedt, *Drug Discovery Today* **2011**, *16*, 569.
- [33] R. Weissleder, *Nat. Biotechnol.* **2001**, *19*, 316.
- [34] N.-N. Dong, M. Pedroni, F. Piccinelli, G. Conti, A. Sbarbati, J. E. Ramírez-Hernández, L. Martínez Maestro, M. C. Iglesias-de la Cruz, F. Sanz-Rodríguez, A. Juarranz, F. Chen, F. Vetrone, J. A. Capobianco, J. G. Solé, M. Bettinelli, D. Jaque, A. Speghini, *ACS Nano* **2011**, *5*, 8665.
- [35] R. Mohr, K. Kratz, T. Weigel, M. Lucka-Gabor, M. Moneke, A. Lendlein, *Proc. Natl. Acad. Sci. USA* **2006**, *103*, 3540.
- [36] C.-T. Lin, K.-C. Liu, *Int. Commun. Heat Mass Transfer* **2009**, *36*, 241.